

# An enhanced multi-position calibration method for consumer grade inertial measurement units applied and tested

Tuukka Nieminen, Jari Kangas, Saku Suuriniemi and Lauri Kettunen

Tampere University of Technology, Electromagnetics, P.O. Box 692, FI-33101  
Tampere, Finland

E-mail: [tuukka.nieminen@tut.fi](mailto:tuukka.nieminen@tut.fi)

**Abstract.** An accurate inertial measurement unit (IMU) is a necessity when considering an inertial navigation system capable of giving reliable position and velocity estimates even for a short period of time. However, even a set of ideal gyroscopes and accelerometers does not imply an ideal IMU if its exact mechanical characteristics (i.e. alignment and position information of each sensor) are not known.

In this paper, the standard multi-position calibration method for consumer grade IMUs using a rate table is enhanced to exploit also the centripetal accelerations caused by the rotation of the table. Thus, the total number of measurements rises, making the method less sensitive to errors and allowing use of more accurate error models. As a result, the accuracy is significantly enhanced, while the required numerical methods are simple and efficient. The proposed method is tested with several IMUs and compared to existing calibration methods.

*Keywords:* Multi-position calibration, inertial measurement unit, rate table, centripetal acceleration

## 1. Introduction

An *inertial measurement unit* (IMU) is the part of an inertial navigation system that provides the measurement data. A typical IMU consists of accelerometers and gyroscopes measuring accelerations and angular velocities which have to be numerically integrated to get the position estimates. Consequently, inertial measurement systems are very sensitive to measurement errors, which we can significantly decrease by means of calibration.

We classify the measurement errors of the IMU into two different categories:

- (i) The errors caused by the unknown mechanical characteristics of the IMU.
  - An uncalibrated IMU is assumed to provide us with specific force and angular rate measurements in an orthogonal basis. In practice, an IMU never yields measurements in an orthogonal basis as such. This is due to inevitable imperfections in the manufacturing process of the IMU.
  - The accelerometers are assumed to measure the specific force of a single point of the IMU. Because of the physical size of the accelerometers, they will measure the specific forces of different points. This is sometimes called the "size effect" [1, 2].

To compensate for these effects, one needs to find the measurement axes of the sensors and the locations of the accelerometers with respect to a chosen point. These errors will be present regardless of the quality of the employed sensors.

- (ii) The errors caused by individual sensors within the IMU.
  - There are both stochastic and deterministic errors present in the data given by a single sensor. The purpose of calibration is to compensate for the most significant deterministic error sources. The most commonly encountered error sources include bias, scale factor and cross-correlation errors. In addition, consumer grade gyroscopes are typically sensitive to linear accelerations [1].

### 1.1. Background

Multi-position calibration is a well-known and a widely employed calibration method. It is based on the idea of keeping the IMU in different positions with respect to the local gravitational acceleration and the angular rate of the Earth [1, 3, 4]. With several independent measurements, it is possible to find the most important error terms of the IMU. Due to the relatively large gravitational acceleration ( $\approx 9.80 \text{ m/s}^2$ ), this method can be applied to practically any set of three accelerometers. However, the extremely small angular rate of the Earth ( $\approx 4.17 \times 10^{-3} \text{ }^\circ/\text{s}$ ) limits the use of this method only to the very accurate and expensive gyroscopes. With consumer grade gyroscopes, the required reference signals must be obtained by another means.

Considering the calibration of accelerometers, the majority of the proposed methods are based on the basic idea of the multi-position calibration method: In every position, the magnitude of the specific force should be equal to the local gravitational acceleration

[3, 5–12]. While the exploited calibration methods and sensor error models have been essentially the same, much progress is achieved in making the required calibration equipment less expensive and thus more suitable for calibration of consumer grade accelerometers [5, 7, 9, 10]. The calibration of redundant sensor configurations is considered in [8, 9].

The basic problem of the calibration methods relying on the gravitational acceleration is the limited magnitude of the reference signals. In practice, also the amount of linearly independent measurements is limited in order to keep the method simple. To overcome these limitations, also some dynamic calibration methods have been suggested. These include the use of a three-dimensional vibration generator [20] and the centripetal accelerations caused by a pendulum [21]. The method considered in [20] gives a possibility to consider also frequency-dependent errors, but requires costly equipment. In the method considered in [21], the rotation radii must be provided and the reference angular rates are computed by numerically differentiating the angle data of the pendulum given by an encoder.

In addition to gyroscope-based inertial measurement units, it is possible to design a gyroscope-free IMU (or GF-IMU). It is based solely on a number of accelerometers mounted on a rigid body. Recent discussion of GF-IMU design can be found from [13–16]. A typical calibration procedure for a GF-IMU is based on the multi-position calibration [14, 16–18] and possibly to a dynamical test making it possible to determine also the locations of the accelerometers [18]. The main motivation for developing such an instruments has been the lack of affordable and reasonably accurate gyroscopes [14, 15]. The disadvantages include the inherently larger size of any reasonably accurate GF-IMU as compared to gyroscope-based IMUs and the degraded measurement accuracy due to indirect measurement of the angular velocity. Furthermore, at the present moment, there are several gyroscopes of fair price-quality ratio available from many manufacturers. In addition to typical "yaw-rate gyros", there is a growing number of devices measuring also the other two directions when mounted on the same circuit board.

Some methods to calibrate consumer grade gyroscopes are considered in [5, 9, 21]. In [9], the required rotations are performed on a rate table operated by hand. Because of this, the true angular rate is unknown and an additional rotations with known rotation angle are required to determine the scale factors. In [5], the calibration is based on multi-position calibration performed on a rate table with known angular rates. Similarly in [21], the numerically computed angular rates of the pendulum can be directly exploited in the calibration. In these studies, the exploited sensor error model has been essentially the same, where g-sensitivity of the gyroscopes is not taken into account.

A totally different kind of an approach is to calibrate the IMU while on the move, using additional information acquired for example, from a GPS system. These methods are well exploited for example, in [1, 2, 4, 22, 23] and are not considered here.

### 1.2. Goal of this study

We consider the calibration of IMUs performed on a low cost rate table. Methodologically, the most relevant sources of this work are [5, 21]. Both consider the calibration of consumer grade IMUs containing three accelerometers and gyroscopes. We will combine the basic ideas of these studies and make some important generalizations and additions to the methods considered therein.

We propose a method that is based on multi-position calibration generalized to exploit the large range of centripetal accelerations caused by different rotation rates of the rate table. As a result,

- the amount of measurement data increases and the calibration procedure becomes less sensitive to errors,
- we can exploit more accurate error models than the ones used in the referred studies,
- it is possible to calibrate the IMU for a certain dynamical range.

The basic idea of the proposed calibration method is to compensate simultaneously for a number of different error sources instead of seeking every modeled error term separately. That is, we will not give a specific meaning to each parameter within the error model, but rather concentrate on compensating for them. The gain of this approach will realize below as somewhat simpler mathematical treatment and more importantly, efficient calibration method based on well-known and widely exploited mathematical tools. If considered necessary, it is just a question of interpretation to distinguish specific error terms from the computed results (as will be discussed later on).

Formally said, the proposed calibration method is based on affine [24] inputs: The reference accelerations contain a constant gravitational acceleration term and a centripetal acceleration term, which is a linear function of the rotation radii. Correspondingly, we model the errors of the accelerometer and gyroscope triads as affine functions. That is, the calibrated output of the sensor triad is modeled by a constant term added to a linear function of the raw sensor output.

Although one is in many cases well aware of the exact type of the sensors within the IMU, the proposed method is also well suited for situations where this is not true. As the calibration methods does not require any specific prior knowledge of the sensors or their locations and directions within the IMU, it can be considered as a black box.

In order for any kind of a calibration method to be useful in practice, it should contain some kind of checks with which one can reliably make sure that the calibration was successful. Along with some standard tools for controlling the quality of the calibration, we introduce a new kind of a control quantity. This is the rotation radius needed to exploit centripetal accelerations. As it could be a difficult task to measure this externally with adequate accuracy, we leave it for the calibration routine to determine. This value is then used as a control quantity, whose approximate value we can easily measure *independently from the calibration routine*.

We will focus especially on the calibration of consumer grade inertial sensors. The practical issues of the actual calibration procedure, such as the accuracy of the reference

data, are emphasized. Throughout the paper, we assume that the IMU is stable over time. This is to say, the effect of temporal instability is assumed to be negligible as compared to the other error sources. While this might sound like a major disadvantage for a calibration method consumer grade sensors with known problems with temporal stability, it actually is not: The possible temporal instability can be compensated by occasionally comparing the output of the sensors when they are known to be in the same position.

### 1.3. Some remarks

Before going on, let us introduce a few central terms. In this context, *error model* is a bijective relation between the raw and the calibrated output of the sensors. Construction of this relation includes both *calibration* and *compensation*. Calibration means that a certain change in the raw output of a certain sensor is related to a certain change in the input [1]. Compensation stands for correcting a number of deterministic errors present in the measurements [1].

This text is organized as follows: In section two, the error models for an accelerometer and a gyroscope triad are presented. The calibration setup will be discussed in section three. The calibration procedure and the underlying formalism are presented in section four. Test results are discussed in section five before the conclusions in section six. Some technical details considering the accuracy of the rate table are discussed in appendices A and B.

## 2. Error models

In this section, we will derive the error models mapping the raw output of the sensors to the calibrated output of the IMU. The aim is to find such a mapping for a certain IMU that minimizes the difference between the actual input and the calibrated output of the IMU (the exact meaning of this is explained later on). The raw output of the IMU is assumed to be a set of AD-converted voltages, naturally expressed as bits. Thus, there is no need to convert the measurements into some more meaningful units prior to applying the constructed error model. Observe that the error model also takes the deterministic errors caused by the interface electronics of the IMU into account. Hence, the calibration should be performed with the same interface electronics as used in the actual measurements.

The calibrated accelerometer and gyroscope outputs given by the IMU are expressed as real-valued vectors  $\mathbf{a} \in \mathbb{R}^3$  and  $\boldsymbol{\omega} \in \mathbb{R}^3$ , respectively. Vectors  $\mathbf{a}$  and  $\boldsymbol{\omega}$  are both given in the standard (orthogonal & right-handed) basis, defined by the calibration system (as will be discussed in section three). The raw accelerometer and gyroscope outputs of the sensors can be readily interpreted as real-valued vectors  $\hat{\mathbf{a}} \in \mathbb{R}^3$  and  $\hat{\boldsymbol{\omega}} \in \mathbb{R}^3$ , respectively. Vectors  $\hat{\mathbf{a}}$  and  $\hat{\boldsymbol{\omega}}$  are given in a basis characteristic to a certain sensor triad within a certain IMU.

Now, let  $\mathbf{S}_a \in \mathbb{R}^{3 \times 3}$  be a diagonal matrix containing the scale factor errors,  $\mathbf{M}_a \in \mathbb{R}^{3 \times 3}$  a skew-symmetric matrix containing the misalignment and cross-coupling errors,  $\mathbf{b}_a \in \mathbb{R}^3$  the bias vector and  $\mathbf{w}_a \in \mathbb{R}^3$  normally distributed, zero-mean measurement noise. Then, a commonly exploited (e.g. [1, 23]) error model for the accelerometers is<sup>‡</sup>

$$\hat{\mathbf{a}} = \mathbf{S}_a \mathbf{a} + \mathbf{M}_a \mathbf{a} + \mathbf{b}_a + \mathbf{w}_a. \quad (1)$$

In a similar fashion, a commonly exploited ([1, 23]) error model for the gyroscopes is

$$\hat{\boldsymbol{\omega}} = \mathbf{S}_\omega \boldsymbol{\omega} + \mathbf{M}_\omega \boldsymbol{\omega} + \mathbf{B}_\omega \mathbf{a} + \mathbf{b}_\omega + \mathbf{w}_\omega, \quad (2)$$

where  $\mathbf{B}_\omega$  describes the g-dependency of the gyroscopes [1].

Keeping (1) in mind, consider equation

$$\hat{\mathbf{a}} = \mathbf{A} \mathbf{a} + \mathbf{b}, \quad (3)$$

where  $\hat{\mathbf{a}} \in \mathbb{R}^3$ ,  $\mathbf{A} \in \mathbb{R}^{3 \times 3}$ ,  $\mathbf{a} \in \mathbb{R}^3$  and  $\mathbf{b} \in \mathbb{R}^3$ . It is not hard to see that (3) is actually the deterministic part of (1), where  $\mathbf{A}$  contains the scale factors, misalignment and cross-correlation terms for each individual sensor along with other possible corrections which can be represented as a constant matrix. Vector  $\mathbf{b} \in \mathbb{R}^3$  contains the constant bias terms of each sensor. Correspondingly for the gyroscopes, consider equation

$$\hat{\boldsymbol{\omega}} = \mathbf{C} \boldsymbol{\omega} + \mathbf{d} + \mathbf{E} \mathbf{a}, \quad (4)$$

where  $\hat{\boldsymbol{\omega}} \in \mathbb{R}^3$ ,  $\mathbf{C} \in \mathbb{R}^{3 \times 3}$ ,  $\boldsymbol{\omega} \in \mathbb{R}^3$ ,  $\mathbf{d} \in \mathbb{R}^3$  and  $\mathbf{E} \in \mathbb{R}^{3 \times 3}$ . In (4)  $\mathbf{C}$  has a similar meaning than  $\mathbf{A}$  in (3),  $\mathbf{d}$  contains the constant bias terms and  $\mathbf{E}$  takes the g-dependency of the gyroscopes into account.

While (3) and (4) are in a convenient form considering the calibration, they are not in a convenient form to be readily exploited by the inertial navigation system. For that, we need to explicitly solve  $\mathbf{a}$  and  $\boldsymbol{\omega}$  from the equations, which yields

$$\mathbf{a} = \mathbf{A}^{-1} (\hat{\mathbf{a}} - \mathbf{b}) \quad (5)$$

$$\boldsymbol{\omega} = \mathbf{C}^{-1} (\hat{\boldsymbol{\omega}} - \mathbf{d} - \mathbf{E} \mathbf{a}). \quad (6)$$

In order to (5) and (6) make sense, matrices  $\mathbf{A}$  and  $\mathbf{C}$  must be invertible, which are necessary conditions for the error models to be bijective relations.

As the formed error models (3) and (4) are clearly affine, they obviously can not compensate for nonlinear errors present in a real situation. However, the constructed error models will be able to compensate for the major error sources of a typical IMU like the misalignment error, scale factor error and constant bias error. Notice that the actual heading of each sensor and the order in which they are given in  $\hat{\mathbf{a}}$  and  $\hat{\boldsymbol{\omega}}$  will not matter as long as the measurement axes are not in the same plane. Thus, it is also possible to consider a certain IMU as a black box without further knowledge about the contents of the IMU.

<sup>‡</sup> As we are dealing with real measurement data, there will always be some errors present that are unaccounted for. For the sake of readability, we decided not to include an error term in each approximate equation, but to overload the usage of equals sign a bit: We use equals sign also in situations, where it strictly speaking should not be used. We are, however, sure that the exact meaning of each equation becomes evident from the context.

### 3. Calibration system

In this section, the practical issues concerning the calibration system are discussed. In addition to general design rules, some remarks of the constructed calibration system are discussed to get an overall idea of the attainable level of accuracy.

As consumer grade gyroscopes are typically not sensitive enough to measure Earth's angular rate, reference signals must be provided by another means. For this, a rate table with a user-controlled angular rate is used (see figure 1) [5, 8, 9]. While calibrating the gyroscopes, it is also convenient to provide accelerometers a number of reference measurements. This is done by using the accelerations created by the rotation along with the gravitational acceleration present in the measurements [21].

While concentrating on consumer grade sensors, the reference signals are not required to be exactly known. Hence, it is safe to drop out a number of factors like Earth's angular rate, Coriolis force (caused by the rotation of the Earth) and the changing rotation radius as a function of the angular rate (only open-loop sensors are subject to this). The effects of these will be negligible as compared to the overall accuracy of the sensors [26].

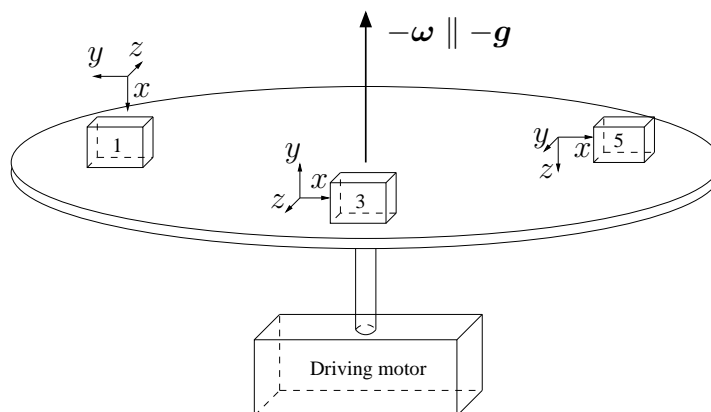


**Figure 1.** Schematic drawing of a rate table, where three different IMU positions (1, 3 and 5; see figure 2) are displayed.

For the calibration system, the critical requirement is that the driving motor of the rate table is able to maintain a *constant angular rate* for a predetermined time (typically, a few seconds). There are several important reasons for this:

- mean angular velocity over a longer period of time can be easily measured (see below) with an accuracy superior to the accuracy of a momentary value [26]
- the effects of the vibration present in a low-cost rate table can be significantly reduced by taking the mean of the output over a longer period of time
- inherent delays in any inertial sensor do not affect the measurements.

In the constructed system, the realized angular rates are measured using an analog optical fork sensor, the output of which is recorded with a sampling frequency  $f = 20$

kHz. In addition, a plate is attached to the rotating table cutting off the optical signal once per a revolution. Measurement error of this kind of a device is analyzed in appendix A. With  $k = 10$ , for example, any mean angular velocity up to  $1000^\circ/\text{s}$  can be measured with an accuracy better than  $5 \times 10^{-4}$  degrees per second. That is, with an accuracy that makes the neglected rotation of the Earth the limiting factor. The error in the reference accelerations are analyzed in appendix B. With the given level of accuracy in the angular rates, the accuracy of the reference accelerations is in practice characterized by the size of the IMU, which is discussed in the next section.

The rate table should be mounted horizontally in such a way that the gravitational acceleration will be perpendicular to the plane of the table. Fortunately, the system is not very sensitive to small mounting errors, since even an easily observed mounting error of  $1^\circ$  will only cause  $\approx 1.5$  mg error in the value of the gravitational acceleration. Moreover, other error components cancel out when the measurement data is averaged over several full revolutions of the table. In the constructed calibration system, the mounting error was less than 0.1 degrees. Thus, in practice, the error in the gravitational acceleration is caused only by the limited accuracy of the externally measured reference value.

To cover all six degrees of freedom, it is required that the IMU is rotated in more than one position. The minimum amount of different positions is three, with every axis of the IMU pointing once out of the plane. In this context, we will consider that the IMU can be positioned in total of six different positions. This amount of positions was chosen to cover positive and negative axis of each sensor. These positions are demonstrated in figure 2 along with the directions of the reference measurements  $\mathbf{g}$  (gravitational acceleration),  $\mathbf{a}_c$  (centripetal acceleration) and  $\boldsymbol{\omega}$  (angular velocity).

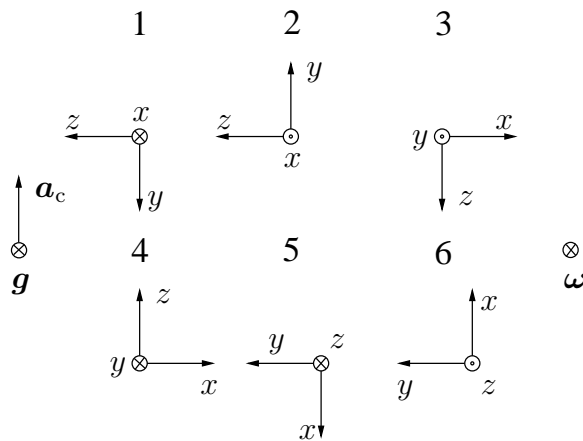


**Figure 2.** Six IMU positions shown by the directions of each orthogonal axis of the calibrated IMU along with the reference measurements. Dot in a circle represents a vector toward the reader and a cross in a circle represents a vector away from the reader.

As suggested by figure 2, all of the six IMU positions are interpreted in such a way that certain axes of the calibrated IMU are collinear with the directions of the reference



measurements. Because of this, the coordinates of the calibrated measurements are actually defined by the calibration system rather than the IMU. Notice that it is only assumed that the different IMU positions are orthogonal with respect to each other, with no requirements for the absolute positions. In the constructed calibration system, the jig used to attach the IMU to the rate table is constructed using precision tools. Thus, the orthogonality of different positions will not be an issue.

For future reference, let us denote the total number of angular rates used to calibrate gyroscopes by  $N$ . Respectively, let the total number of angular rates used to calibrate accelerometers be  $M$ . With a total of six different positions, we have  $6 \times N$  and  $6 \times M$  measurements per single axis of the IMU. Notice that  $M$  and  $N$  represent the set of rotation rates one plans to use in the computations, which is generally different than the set of actual rotation rates. In practice this could, for example, mean that one wishes to find several calibration functions, each of which is optimized to certain range of inputs.

#### 4. Calibration procedure

In this section, details of the calibration procedure are discussed. To give an overview of the calibration procedure, let us first state the recipe for it as follows:

- (i) Gather the needed data by rotating the IMU with a number of different angular rates for all six positions seen in figure 2.
- (ii) Construct a set of numerical equations for the calibration parameters according to (3) and (4).
- (iii) Solve the constructed, generally overdetermined and hence an approximative set of equations.
- (iv) Conduct a reality check for the computed results by comparing a number of control quantities against known reference values.

As step one is already clear, we will now discuss steps 2, 3 and 4 in detail.

##### 4.1. Step two: constructing the needed equations

Recall the discussion about the physical size of the IMU in section 1 and appendix B. There are two ways the physical size of the IMU will affect the output of an accelerometer located at a point different than the chosen origin of the IMU:

- tangential acceleration caused by the angular acceleration and
- centripetal acceleration caused by the angular velocity.

As the calibration procedure exploits only constant angular rates, the observed tangential acceleration will be zero. Thus, we do not need to take this into account while constructing the needed equations. Furthermore, in a typical situation, the effects of tangential acceleration are difficult to compensate for, since the angular acceleration is unknown.

**Table 1.** Reference measurements for the accelerometers and gyroscopes when rotating the IMU in the six positions.

| Position | Reference measurements |                       |                       |                 |                 |                 |
|----------|------------------------|-----------------------|-----------------------|-----------------|-----------------|-----------------|
|          | Acceleration           |                       |                       | Angular rate    |                 |                 |
|          | $x$                    | $y$                   | $z$                   | $x$             | $y$             | $z$             |
| 1        | $-g$                   | $-\omega_{1,j}^2 r_1$ | 0                     | $\omega_{1,j}$  | 0               | 0               |
| 2        | $g$                    | $\omega_{2,j}^2 r_2$  | 0                     | $-\omega_{2,j}$ | 0               | 0               |
| 3        | 0                      | $g$                   | $-\omega_{3,j}^2 r_3$ | 0               | $-\omega_{3,j}$ | 0               |
| 4        | 0                      | $-g$                  | $\omega_{4,j}^2 r_4$  | 0               | $\omega_{4,j}$  | 0               |
| 5        | $-\omega_{5,j}^2 r_5$  | 0                     | $-g$                  | 0               | 0               | $\omega_{5,j}$  |
| 6        | $\omega_{6,j}^2 r_6$   | 0                     | $g$                   | 0               | 0               | $-\omega_{6,j}$ |

Centripetal acceleration caused by nonzero  $\delta \mathbf{r}$  seen in appendix B is, however, observed. Thus, in general, each accelerometer has a unique rotating radius for each of the six positions of the IMU. For a "small-sized" consumer grade IMU, it is sometimes reasonable to assume that the effects caused by  $\delta \mathbf{r}$  are negligible as compared to other sources of error. That is, the error estimates given in appendix B give values smaller than the expected errors in the calibrated sensors. When this is the case, we will only need one radius for each position. However, given a certain IMU, it is a task far from trivial to specify these externally with adequate accuracy. Thus, we leave these for the calibration routine to determine. This way, we do not need to commit to the location of the actual origin of the IMU in any way. Instead, we can leave it up to the calibration routine to specify the location of an origin minimizing the error caused by ignoring the size of the IMU. In the following treatment, it is assumed that the IMU is small. The presented methods can be readily generalized to the situation where this is not the case.

From figure 2, one will end up with the reference measurements seen in table 1. In the table,  $g$  is the local gravitational acceleration,  $\omega_{i,j}$  angular velocity of step  $j$  while the IMU is in position  $i$  and  $r_i$  rotation radius for position  $i$ .

Now, let us denote the reference acceleration of the step  $j \in [1, \dots, M]$  of the position  $i \in [1, \dots, 6]$  by  $\mathbf{a}_{i,j}(r_i)$  and the respective measurements  $\hat{\mathbf{a}}_{i,j}$ . By recalling (3) and defining a  $3 \times 9$  matrix

$$\mathbf{R}_a(i, j, r_i) = \begin{bmatrix} \mathbf{a}_{i,j}^T(r_i) & \mathbf{0}^T & \mathbf{0}^T \\ \mathbf{0}^T & \mathbf{a}_{i,j}^T(r_i) & \mathbf{0}^T \\ \mathbf{0}^T & \mathbf{0}^T & \mathbf{a}_{i,j}^T(r_i) \end{bmatrix}, \quad (7)$$

we get an equation

$$\begin{bmatrix} \mathbf{R}_a(i, j, r_i) & -\mathbf{I} \end{bmatrix} \mathbf{x} = \hat{\mathbf{a}}_{i,j} \quad (8)$$

for vector  $\mathbf{x} \in \mathbb{R}^{12}$  containing the elements of  $\mathbf{A}$  and  $\mathbf{b}$  in row-wise order. Matrix  $\mathbf{I}$  is a  $3 \times 3$  identity matrix. Clearly, (8) is now a nonlinear equation because of the terms  $r_i$  in the coefficient matrix. When considering a single measurement  $\hat{\mathbf{a}}_{i,j}$ , (8) is

underdetermined with only 3 independent measurements for 18 unknowns. By stacking equations (8) for all  $i$  and  $j$ , one will get a system with a total of  $3 \times 6 \times M$  equations for 18 unknowns. From this, it is clear that  $M$  must be at least 1 to have a well posed problem. In practice, with several error sources unaccounted for,  $M$  should be larger thus making the resulting nonlinear equation overdetermined.

For the gyroscopes, let us first define a  $3 \times 9$  matrix

$$\mathbf{R}_\omega(i, j) = \begin{bmatrix} \boldsymbol{\omega}_{i,j}^T & \mathbf{0}^T & \mathbf{0}^T \\ \mathbf{0}^T & \boldsymbol{\omega}_{i,j}^T & \mathbf{0}^T \\ \mathbf{0}^T & \mathbf{0}^T & \boldsymbol{\omega}_{i,j}^T \end{bmatrix} \quad (9)$$

containing the reference measurements. With a treatment similar to the previous paragraph and recalling (4), one will end up with an equation

$$\begin{bmatrix} \mathbf{R}_\omega(i, j) & -\mathbf{R}_a(i, j, r_i) & -\mathbf{I} \end{bmatrix} \mathbf{y} = \hat{\boldsymbol{\omega}}_{i,j} \quad (10)$$

for vector  $\mathbf{y} \in \mathbb{R}^{21}$  containing the elements of  $\mathbf{C}$ ,  $\mathbf{E}$  and  $\mathbf{d}$  in row-wise order. Again, when considering a single measurement  $\hat{\boldsymbol{\omega}}_{i,j}$ , (10) is underdetermined with only 3 independent measurements for 21 unknowns. In this case, by stacking equations (10) for all  $i$  and  $j$ , we end up with a system with a total of  $3 \times 6 \times N$  linear equations for 21 unknowns. The fact that (10) is linear is based on the assumption that (8) is already solved, giving access to parameters  $r_i$ .

#### 4.2. Step three: solving the constructed equations

In the previous section we constructed equations for the calibration functions we were looking for. As seen above, the equation for the accelerometers is nonlinear. Hence, we will have to use a nonlinear optimization routine to find out an optimal solution in some sense.

Let us denote the nonlinear system for the calibration parameters of the accelerometer triad in a form  $\mathbf{z} = \mathbf{h}(\mathbf{x})$ . Now we can write its residual  $\mathbf{p}(\mathbf{x})$  as

$$\mathbf{p}(\mathbf{x}) = \mathbf{h}(\mathbf{x}) - \mathbf{z}. \quad (11)$$

A typically used criteria for an optimal solution is the minimum of the quadratic form  $\|\mathbf{p}(\mathbf{x})\|^2$ :

$$\tilde{\mathbf{x}} = \operatorname{argmin} \mathbf{p}(\mathbf{x})^T \mathbf{p}(\mathbf{x}). \quad (12)$$

We will exploit Gauss-Newton to solve this nonlinear optimization problem [27]. For this, we will need the Jacobian of the function  $\mathbf{h}(\mathbf{x})$ , which we can compute using (8) and table 1. The algorithm goes as follows [27]:

- (i) Choose  $\mathbf{x}_0$  and a suitable end criteria  $\delta$ . Set  $n = 0$ .
- (ii) Compute  $\mathbf{J}_n = \frac{d}{d\mathbf{x}} \mathbf{h}(\mathbf{x}_n)$ .
- (iii) Compute  $\mathbf{x}_{n+1} = \mathbf{x}_n - (\mathbf{J}_n^T \mathbf{J}_n)^{-1} \mathbf{J}_n [\mathbf{h}(\mathbf{x}_n) - \mathbf{z}]$ .
- (iv) If  $\|\mathbf{x}_{n+1} - \mathbf{x}_n\| \geq \delta$ , set  $n = n + 1$  and continue from step 2.

A suitable stopping criterion is the step length  $\|\mathbf{x}_{n+1} - \mathbf{x}_n\| < \delta$ .

As seen from the algorithm above, one must provide an initial guess  $\mathbf{x}_0$ . For a general nonlinear optimization problem, this is a nontrivial task having a great effect on the solution speed and possibly on the "optimal" result obtained [27]. When this was tested using the test data considered later in this text, the choice of initial guess (provided that  $\mathbf{J}_n^T \mathbf{J}_n$  is nonsingular) did not have any influence on the given solution or the solution speed. In each case, the optimization routine found the solution after a few iterations.

In case of the gyroscopes, an approximative solution can be achieved simply by computing a least squares solution for  $\mathbf{y}$ . When constructing the equation, needed  $\mathbf{a}_{i,j}(r_i)$  can be provided by the known reference signals. Provided, of course, that the rotation radii are already known.

In some cases, one might have better knowledge about the reliability of the measurements or even knowledge about the correlation of different measurements. There is no problem in using readily available generalizations of the presented solution schemes to these situations [27]. In fact, as the proposed method is based on averaging the collected data, the variance of each measurement could be readily estimated as well.

#### 4.3. Step four: control quantities

In any practical situation, one should have some confidence about how successful the calibration was, before a particular IMU can be considered as ready to be used. For this, one can readily compute a number of control quantities right after the actual computation is done.

For an overall view about the sensitivity of the method to measurement errors, one can compute the condition numbers for the constructed matrices. For general non-square matrices, it is defined to be the condition number of the product of the transpose of the matrix and the matrix itself [28]. If reasonable values for the rotation radii are available before the computation, this check can be done before the actual computation takes place. Similarly, it is also possible to estimate the sensitivity of a particular IMU to measurement errors by computing the condition numbers of  $\mathbf{A}$  and  $\mathbf{C}$ .

For a quantity describing how well the calibration function of the accelerometers fits the measurement data, one can estimate the standard deviation  $s_a$  of the residual (11) as follows [29]:

$$s_a = \sqrt{\frac{\mathbf{p}(\mathbf{x})^T \mathbf{p}(\mathbf{x})}{(3 \times 6 \times M) - 1}}. \quad (13)$$

This can be computed for the gyroscopes as well ( $s_g$ ), by replacing  $\mathbf{p}(\mathbf{x})$  with the residual of (10) and  $M$  by  $N$ .

In case of accelerometers, matrix  $\mathbf{J}_n^T \mathbf{J}_n$  evaluated at the optimum can be used to estimate the covariance matrix of the standard errors of the computed parameters [10, 30]. This gives a possibility to compute confidence intervals for the estimated

parameters, if considered necessary. For the gyroscopes, this can be achieved by analyzing the coefficient matrix of the normal equations.

All of the control quantities provided above are standard methods in measurement science, which can be readily used to gain information about the calibration and goodness of fit. They can be readily used to compare different measurements, but to gain useful information about the absolute accuracy, knowledge of the actual sensors within the IMU is required. In typical situations this is acceptable, but this is not the case considering the black box situation. In this case, the computed rotation radii provide a suitable method to decide whether the calibration was successful or not: Consider, for example, that the value of the gravitational acceleration is given in units of g instead of  $\text{m/s}^2$ . As such, this is only going to scale the computed parameters differently, and will be visible only if the specifications of the used sensors are known. However, this error will be immediately seen in the values of the computed rotation radii.

## 5. Test results

The proposed calibration method was tested with a total of eight hand-made IMUs. All IMUs were constructed in the same way, where each individual sensor was supposed to measure parallel to  $x$ ,  $y$  or  $z$  direction seen in figure 1. The test results are divided into three parts. The first part shows the differences in the calibration characteristics. The second part shows the actual difference between a calibrated and uncalibrated IMU as seen by the error models. Finally, the third part shows the differences in actual measurements. While a real navigation test is not included, the difference made by the calibration is clearly shown by the provided results.

The calibrations were performed using a 16-bit AD-converter to store the signals given by the IMU. 12 g accelerometers [31] were used along with 300  $^\circ/\text{s}$  gyroscopes [32]. For the accelerometers it holds that  $M = 30$  (recall that  $M$  is the number of the used angular rates to calibrate the accelerometers) and  $N = 10$  for the gyroscopes. The used rotation rates were designed to follow approximately the following plan: (30–300)  $^\circ/\text{s}$  with 30  $^\circ/\text{s}$  increments (up to 1 g), (1–3) g with 0.25 g increments, (3–6) g with 0.5g increments and (6–12) g with 1 g increments (depending on the actual rotation radius). The size of the IMU was confirmed not to cause significant errors by simulations, and thus it was possible to use the approximation  $\delta r \approx 0$ .

### 5.1. Comparison between different IMUs

Let us next present a few characteristics (described in the section 4.3) of each test is collected to table 2.

Because the measurements are expressed in bits, the most natural unit of parameters  $s_a$  and  $s_g$  seen in table 2 would also be bits. For clarity, however, they are converted to more meaningful units using the rule: 100 bits correspond 50 mg for the accelerometers and 1.6  $^\circ/\text{s}$  for the gyroscopes. These values are based on the scale

**Table 2.** Calibration characteristics of a total of eight hand-made IMUs.

| IMU | Accelerometers |           |           |           |           |           |           | Gyros |
|-----|----------------|-----------|-----------|-----------|-----------|-----------|-----------|-------|
|     | $s_a$          | $r_1$     | $r_2$     | $r_3$     | $r_4$     | $r_5$     | $r_6$     | $s_g$ |
| 1   | 30.7           | 23.8±0.28 | 26.6±0.32 | 24.9±0.30 | 25.7±0.31 | 24.5±0.29 | 25.9±0.31 | 0.32  |
| 2   | 33.7           | 23.8±0.31 | 26.7±0.35 | 24.8±0.32 | 25.6±0.33 | 24.6±0.32 | 25.8±0.33 | 0.33  |
| 3   | 33.2           | 23.7±0.31 | 26.6±0.34 | 24.9±0.32 | 25.7±0.33 | 24.6±0.31 | 25.9±0.33 | 0.34  |
| 4   | 32.9           | 23.8±0.30 | 26.7±0.34 | 24.9±0.32 | 25.7±0.33 | 24.6±0.31 | 25.8±0.33 | 0.40  |
| 5   | 31.0           | 23.8±0.29 | 26.5±0.32 | 24.9±0.30 | 25.7±0.31 | 24.4±0.29 | 25.8±0.31 | 0.33  |
| 6   | 31.0           | 23.7±0.28 | 26.7±0.32 | 24.9±0.30 | 25.7±0.31 | 24.5±0.29 | 25.9±0.31 | 0.37  |
| 7   | 32.9           | 23.7±0.30 | 26.8±0.34 | 24.9±0.32 | 25.5±0.33 | 24.5±0.31 | 25.8±0.32 | 0.31  |
| 8   | 33.2           | 23.7±0.31 | 26.7±0.34 | 24.8±0.32 | 25.7±0.33 | 24.5±0.31 | 25.7±0.33 | 0.32  |

Radii  $r_i$  are expressed in centimeters.

Standard deviations  $s_a$  and  $s_g$  are expressed in mg and °/s, respectively.

± signs indicates 95% confidence intervals of the radii estimated using  $s_a \sqrt{\text{trace} \left( \left( \mathbf{J}_n^T \mathbf{J}_n \right)^{-1} \right)}$  [30].

factors of the sensors reported in [31] and [32].

From table 2, it is noted that the overall characteristics of the all eight IMUs are close to each other. Knowing that the IMUs are constructed by hand and that the computed radius is just an approximative value for any realistic IMU, the computed radii are consistent, with a typical confidence interval of ±3.1 mm. The typical values for  $s_a$  and  $s_g$  for noncalibrated sensors are not displayed, since the constant bias alone would cause them to be in the order of 0.1 g and 1 °/s, respectively

### 5.2. Comparison of the calibration functions

In this section, the computed error models of the IMU number 1 are discussed in detail. This gives a possibility to compare them against the situation where no calibration can be done. In this case, the values are taken directly from the specifications of the sensors. For clarity, the numerical values represented here are converted to standard units; i.e. voltages, g and degrees / second. Notice, however, that the proposed method does not require this to be done.

In table 3, the parameters for the calibrated output of the accelerometers are shown. In case no calibration is done, matrix  $\mathbf{A}$  is a diagonal matrix having values  $-6.667$  at the diagonal and  $\mathbf{b}$  is a vector consisting of values  $b_i = -2.350$  (i.e. the used accelerometers are set to show zero when placed on the desk). Notice that there is a significant difference between the scale factors given by the manufacturer and the computed ones. This is explained by the fact that the used datalogger had, for some reason, a tendency to underestimate voltages. This does not affect the other results considered in this section: this is why the calibration should be done using the same datalogger that is used to store the data in action. The parameters for the calibrated output of the gyroscopes are shown in table 4. In case no calibration is performed, the scale factor is ±166.667

**Table 3.** Numerical example of the calibration function (3).

| $\mathbf{A}$ [g/V] |        |        | $\mathbf{b}$ [V] |
|--------------------|--------|--------|------------------|
| -6.929             | 0.048  | -0.160 | -2.351           |
| -0.132             | -7.005 | -0.052 | -2.369           |
| -0.024             | 0.160  | -7.020 | -2.350           |

**Table 4.** Numerical example of the calibration function (4).

| $\mathbf{C}$ [°/s/V] |        |        | $\mathbf{E}$ [°/s/g] |        |        | $\mathbf{d}$ [V] |
|----------------------|--------|--------|----------------------|--------|--------|------------------|
| -208.5               | -1.652 | -1.953 | -0.152               | 0.024  | 0.137  | -2.574           |
| 1.051                | -207.6 | -0.601 | 0.194                | -0.051 | -0.163 | -2.464           |
| 2.553                | -0.526 | 208.4  | -0.013               | -0.043 | 0.027  | -2.475           |

depending on the sensor and bias value  $b_i = -2.500$ . As one could expect, the large difference in the scale factors is observed also here.

To give an overall idea about the error models, the diagonal elements of the matrices  $\mathbf{A}$  and  $\mathbf{C}$  correspond to the scale factors of each individual sensor. Provided, of course, that the sensor readings are picked up in a "correct" order. Minus sign in the scale factor simply means that the sensor is upside down. The off-diagonal parameters are caused by the misalignment and the cross-correlation of the sensors. If the off-diagonal terms are interpreted as a consequence of the geometrical alignment error alone, we can easily compute the corresponding error angles: by normalizing each column vector of  $\mathbf{A}$  and  $\mathbf{C}$ , each element of the resulting six vectors is the sine of the respective error angle. For instance, the elements of the first column vector of  $\mathbf{A}$  correspond to angles  $-88.89^\circ$ ,  $-1.09^\circ$  and  $-0.20^\circ$ . The first angle indicates that the corresponding sensor was aligned at an angle  $178.89^\circ$  with respect to the corresponding axis of the IMU.

This kind of a geometrical interpretation can not be made for the matrix  $\mathbf{E}$  representing the dependency of the measured angular rate from the linear acceleration seen in table 4. In this particular case, all the elements of the respective matrix are close to each other indicating that the magnitude of the coupling between linear acceleration and measured angular rate is about the same for all axes.

### 5.3. Comparison of the measurement accuracy

In this section, the gain of the calibration procedure performed to the IMU number 1 is discussed. Notice that the accuracy tests are performed on the same rate table that was used to calibrate data. This was the only possibility to generate accurate reference accelerations up to 12 g and reference angular rates up to 300 °/s, since we did not have the possibility to exploit high accuracy reference sensors. However, the angular rates and accelerations used to demonstrate the accuracy were *not* used in the calibration. Furthermore, the accuracy tests and the calibration routine were run as two separate events. The run-to-run variation of the sensor bias was taken into account by averaging

**Table 5.** Results of the accuracy test performed for the accelerometers of the IMU number 1. The Expected values are the reference accelerations computed with the known values of the rotation radii.

| Expected [g] |        |        | Measured acceleration [g] |        |        |                     |        |        |
|--------------|--------|--------|---------------------------|--------|--------|---------------------|--------|--------|
| $x$          | $y$    | $z$    | Proposed method           |        |        | Six-position method |        |        |
|              |        |        | $x$                       | $y$    | $z$    | $x$                 | $y$    | $z$    |
| -1.000       | -0.007 | 0.000  | -0.991                    | 0.014  | -0.013 | -1.003              | -0.002 | 0.006  |
| 1.000        | 0.007  | 0.000  | 1.008                     | 0.043  | 0.003  | 0.998               | 0.012  | 0.008  |
| 0.000        | 1.000  | -0.007 | 0.015                     | 1.020  | -0.020 | 0.009               | 0.995  | -0.004 |
| 0.000        | -1.000 | 0.007  | 0.013                     | -0.978 | 0.012  | -0.002              | -1.000 | 0.019  |
| -0.007       | 0.000  | -1.000 | 0.005                     | 0.037  | -1.004 | -0.003              | 0.018  | -0.992 |
| 0.007        | 0.000  | 1.000  | 0.038                     | 0.037  | 0.990  | 0.025               | 0.011  | 1.002  |
| -1.000       | -9.096 | 0.000  | -1.007                    | -9.095 | 0.135  | -1.061              | -9.099 | 0.117  |
| 1.000        | 10.172 | 0.000  | 0.988                     | 10.174 | 0.118  | 1.024               | 10.129 | 0.164  |
| 0.000        | 1.000  | -9.517 | -0.071                    | 1.004  | -9.483 | -0.055              | 1.018  | -9.472 |
| 0.000        | -1.000 | 9.840  | -0.061                    | -0.998 | 9.866  | -0.100              | -1.058 | 9.881  |
| -9.371       | 0.000  | -1.000 | -9.358                    | -0.196 | -1.040 | -9.376              | -0.144 | -0.960 |
| 9.921        | 0.000  | 1.000  | 9.927                     | -0.191 | 0.957  | 9.922               | -0.293 | 0.894  |

the output before the accuracy test took place.

In case of the accelerometers, the used sensor error model is identical to the ones used before. Only the calibration method has changed from the basic six-position calibration method to the proposed method. The accuracy of these two methods are compared against the reference accelerations. The positions used for the six-position calibration are the ones used in the proposed method, while the rate table was not rotating. In case of the gyroscopes, we use an error model different from the ones used in the referred studies. Namely, the g-dependent bias is also taken into account. In this case the calibration method is basically the same than the one seen for example, in [5]. The accuracy of the two models are compared against the reference angular rates. The results corresponding to the two choices of error models were both computed using the same measurements.

In table 5, the calibrated results of the accelerometer triad are compared to the reference signals in all six positions seen in figure 2 while the rate table was rotated at two different angular rates. The angular rates were selected in such a way that both ends of the accelerometers dynamic range were covered. The reference signals are seen at the left and the output of the accelerometer triad using the proposed calibration method at the center. The results given by the standard six-position calibration method are seen at the right.

The results given by the standard six-position calibration method are somewhat better whenever the total reference acceleration is close to 1 g. This is expectable since this method uses acceleration up to 1 g, whereas the proposed method uses the whole dynamic range of the accelerometers. With higher accelerations, the proposed



**Table 6.** Results of the accuracy test performed for the gyroscopes of the IMU number 1. The Expected values are the reference rotation rates.

| Expected [ $^{\circ}/s$ ] |        |        | Measured angular rate [ $^{\circ}/s$ ] |        |        |                           |        |        |
|---------------------------|--------|--------|--|--------|--------|---------------------------|--------|--------|
| $x$                       | $y$    | $z$    | Proposed method                        |        |        | Method by Syed et al. [5] |        |        |
|                           |        |        | $x$                                    | $y$    | $z$    | $x$                       | $y$    | $z$    |
| 30.2                      | 0.0    | 0.0    | 30.3                                   | 0.1    | -0.1   | 30.3                      | 0.3    | -0.1   |
| -30.0                     | 0.0    | 0.0    | -30.2                                  | 0.0    | 0.0    | -30.1                     | -0.2   | 0.0    |
| 0.0                       | -29.9  | 0.0    | -0.2                                   | -29.7  | 0.1    | -0.3                      | -29.7  | 0.1    |
| 0.0                       | 29.9   | 0.0    | -0.2                                   | 29.9   | 0.1    | -0.1                      | 29.8   | 0.0    |
| 0.0                       | 0.0    | 29.9   | 0.4                                    | 0.2    | 30.2   | 0.6                       | 0.1    | 30.2   |
| 0.0                       | 0.0    | -29.9  | 0.4                                    | 0.2    | -29.8  | 0.3                       | 0.3    | -29.9  |
| 305.8                     | 0.0    | 0.0    | 306.4                                  | -0.9   | -0.5   | 306.4                     | -1.0   | -0.5   |
| -305.7                    | 0.0    | 0.0    | -305.3                                 | -0.8   | -0.3   | -305.4                    | -0.7   | -0.3   |
| 0.0                       | -305.6 | 0.0    | -0.2                                   | -305.3 | 0.7    | -0.2                      | -305.3 | 0.7    |
| 0.0                       | 305.6  | 0.0    | -0.1                                   | 306.0  | 0.8    | -0.2                      | 306.0  | 0.8    |
| 0.0                       | 0.0    | 305.7  | -0.7                                   | 0.0    | 305.2  | -0.8                      | 0.1    | 305.1  |
| 0.0                       | 0.0    | -305.6 | -0.4                                   | 0.1    | -306.0 | -0.3                      | 0.0    | -306.0 |

calibration method gives a better overall accuracy. This can be verified by computing the value  $s_a$  for the standard six-position calibration method, which gives  $s_a = 80.2$  mg against a typical value of 32 mg obtained with the proposed method. Hence, the proposed calibration method gives better results than the standard six-position calibration, when considering the whole dynamic range of the sensors. One reason for this is that the six-position calibration method relies on extrapolation when applied to sensors with a range exceeding 1 g. Secondly, small alignment errors are not necessarily observable due to the limited sensitivity of the sensors.

For the gyroscopes, more specific calibration results can be found in table 6. The reference and measured angular rates for each six positions are tabulated for two angular rates at the both ends of the dynamic range. The reference angular rate is seen at the left, proposed calibration (with g-dependency) output of the gyroscope triad at the center and output of the method proposed in [5] (without g-dependency) at the right.

In this case, the overall performance of the two calibration functions are close to each other. This is quantified by the value  $s_g = 0.33$   $^{\circ}/s$  for the method where g-dependency is not considered. This is larger than the corresponding value  $s_g = 0.32$   $^{\circ}/s$ , but considering the variation in these values between different IMUs, this is hardly a significant difference. This is explained by the fact that during the test the total acceleration acting upon the IMU was at most 1.2 g, because rotations rates up to 300  $^{\circ}/s$  do not cause centripetal accelerations larger than 0.7 g with the given radii. As table 4 proposes, the difference of the methods should not be that dramatic in these kind of circumstances. Angular velocity of  $[0.0 \ 1110.3 \ 0.0]^T$   $^{\circ}/s$ , on the other hand, causes a total acceleration of  $\approx 10$  g. In this case the angular velocity given by the proposed method is  $[-3.6 \ 484.0 \ 0.5]^T$   $^{\circ}/s$ , and the angular velocity given by

the method proposed by [5] is  $[-5.1 \ 484.2 \ 0.9]^T$  °/s. Obviously, the  $y$ -components are useless in both cases because the rate exceeds the range of the used sensors. In the other components, however, there is a clear improvement over the method proposed in [5].

## 6. Conclusions

With the methods described in this paper, it is possible to enhance the overall accuracy of an IMU to a better level than the standard six-position calibration would allow. In the conducted experiments for accelerometers, for example, the standard deviation of the residual error is 32.0 mg against the value of 80.2 mg acquired using the standard calibration. In case of the gyroscopes, it is demonstrated that under low accelerations, the results are comparable to known calibration methods (residual error 0.32 °/s vs. 0.33 °/s). Under high accelerations, the proposed method can significantly increase the accuracy. This can be achieved without detailed knowledge about the sensors within the IMU, as long as it is capable of measuring general rotations and accelerations. For example, the IMU could include sensors with different dynamic ranges thus causing the scale factors to be different for each axis. One does not need to know this beforehand, as the proposed method does not require any prior knowledge about the parameters to be computed. Using the provided control quantities, it can be easily verified if the calibration process was successful or not. The proposed method also allows one to compute error models specialized in a certain range of inputs, expanding the use of sensors with a fixed range without need for recalibration.

As the focus is on consumer grade IMUs, the used reference angular rates must be provided by a rate table of some sort. However, the design requirements for this are fulfilled without costly and precise equipment, because the calibration process uses only a set of constant angular velocities. A rate table provides a way to perform more complete calibration routines using also the centripetal accelerations as reference accelerations. The rotation radii do not need to be known, as the provided solution method can solve for these along with the actual calibration parameters.

The calibration functions presented here are not the only possible choices, but examples of accurate, but still simple calibration functions. One can also use a different error model important in a particular application, as the total amount of the measurements gives a possibility to do this. While the proposed method is based on the use of affine functions, use of non-affine calibration functions could also be possible at least when good initial guesses are available. Another interesting point is how to exploit redundant sensor configurations. Basically, the proposed method can be readily generalized to these situations, since we would only need to consider rectangular matrices  $\mathbf{A}$ ,  $\mathbf{C}$  and  $\mathbf{D}$  instead of the square ones considered here. This will, however, introduce questions about the uniqueness of the solution, which need to be examined first.

While the provided calibration functions compensate for the main error sources (scale factor, misalignment, cross correlation and bias errors) of consumer grade IMUs, they are simple enough to be used in any INS. This is because only simple matrix

multiplications and vector additions are required, and these can be applied directly to the raw data. However, as the method is based on a relatively simple calibration process, it cannot compensate for more complicated error sources such as run-to-run variations of the biases. When these kind of corrections are necessary, they can be applied to the calibrated output of the IMU.

## References

- [1] Titterton D H and Weston J L 2004 *Strapdown Inertial Navigation Technology (2nd Edition)* (The American Institute of Aeronautics and Astronautics)
- [2] Farrell J A and Barth M 1998 *The Global Positioning System & Inertial Navigation* (McGraw-Hill)
- [3] Grewal M S, Henderson V D and Miyasako R S 1991 Application of Kalman filtering to the calibration and alignment of inertial navigation systems *IEEE Trans. on Automatic Control* **36** 3–13
- [4] Chatfield A B 1997 *Fundamentals of High Accuracy Inertial Navigation* (The American Institute of Aeronautics and Astronautics)
- [5] Syed Z F, Aggarwal P, Goodall C, Niu X and El-Sheimy N 2007 A new multi-position calibration method for MEMS inertial navigation systems *Meas. Sci. Technol.* **18** 1897–1907
- [6] Fong W T, Ong S K and Nee A Y C 2008 Methods for in-field user calibration of an inertial measurement unit without external equipment *Meas. Sci. Technol.* **19** 085202 (11pp)
- [7] Lötters J C, Schipper J , Veltink P H , Olthuis W and Bergveld P 1998 Procedure for in-use calibration of triaxial accelerometers in medical applications *Sensors and Actuators A: Physical* **68** 221–228
- [8] Cho S Y and Park C G 2005 A Calibration Technique for a Redundant IMU Containing Low-Grade Inertial Sensors *ETRI Journal* **27** No 4 418–426
- [9] Myung Hwangbo and Kanade T 2008 Factorization-based calibration method for MEMS inertial measurement unit *IEEE Int. Conf. on Robotics and Automation* 1306–11
- [10] Isaac Skog and Peter Händel 2006 Calibration of a MEMS Inertial Measurement Unit *XVII IMEKO World Congress, September 17-22, Rio de Janeiro (Brazil)*
- [11] Gökçen Aslan and Afşar Saranlı 2008 Characterization and Calibration of MEMS Inertial Measurement Units *16th European Signal Processing Conference, August 25-29, Lausanne (Switzerland)*
- [12] Wu Z C, Wang Z F and Ge Y 2002 Gravity based online calibration for monolithic triaxial accelerometers' gain and offset drift *Proc. of the 4th World Congress on Intelligent Control and Automation, June 10-14, Shanghai (China)*

- [13] Zappa B, Legnani G, van den Bogert A J and Adamini R 2001 On the Number and Placement of Accelerometers for Angular Velocity and Acceleration Determination *Journal of Dynamic Systems* **123** No 3 552–554
- [14] Parsa K, Angeles J and Misra A K 2002 Attitude Calibration of an Accelerometer Array *Proc. IEEE Int. Conf. on Robotics & Automation, May 11-15, Washington DC* **1** 129–134
- [15] Park S, Tan C-W and Park J 2005 A scheme for improving the performance of a gyroscope-free inertial measurement unit *Sensors and Actuators A: Physical* **121** 410–420
- [16] Parsa K and Lasky T A 2007 Design and Implementation of a Mechatronic, All-Accelerometer Inertial Measurement Unit *IEEE/ASME Trans. on Mechatronics* **12** No 6
- [17] Hung C-Y and Lee S-C 2006 A Calibration Method for Six-Accelerometer INS *Int. Journal of Control, Automation, and Systems* **4** No 5 615–623
- [18] Cappa P, Patanè F and Rossi S 2008 Two calibration procedures for a gyroscope-free inertial measurement system based on a double-pendulum apparatus *Meas. Sci. Technol.* **19** 055204 (9pp)
- [19] Kim A and Golnaraghi M F 2004 Initial calibration of an inertial measurement unit using an optical position tracking system *Proc. of Position Location and Navigation Symposium, PLANS, April 2004* 96-101
- [20] Umeda A, Onoe M, Sakata K, Fukushima T, Kanari K, Iioka H and Kobayashi T 2004 Calibration of three-axis accelerometers using a three-dimensional vibration generator and three laser interferometers *Sensors and Actuators A: Physical* **114** 93–101
- [21] Alves J, Lobo J and Dias J 2003 Camera-Inertial Sensor Modeling and Alignment for Visual Navigation *Journal of Machine Intelligence & Robotic Control* **5** No 3 103–111
- [22] Nebot E and Durrant-Whyte H 1999 Initial Calibration and Alignment of Low-Cost Inertial Navigation Units for Land Vehicle Applications *Journal of Robotic Systems* **16** No 2 81–92
- [23] Grewal M S, Weill L R and Andrews A P 2001 *Global Positioning Systems, Inertial Navigation, and Integration* (John Wiley & Sons Inc.)
- [24] Bossavit A 1998 *Computational Electromagnetism* (Academic Press)
- [25] Golub G H and Van Loan C F 1996 *Matrix Computations (3rd Edition)* (The John Hopkins University Press)
- [26] IEEE Aerospace and Electronic Systems Society 2001 *IEEE recommended practice for precision centrifuge testing of linear accelerometers* (The American Institute of Aeronautics and Astronautics)
- [27] Bertsekas D P 1995 *Nonlinear Programming* (Athena Scientific)

- [28] Demmel J W 1997 *Applied Numerical Linear Algebra* (Society for Industrial and Applied Mathematics)
- [29] Rosenkrantz W A 1997 *Introduction to Probability and Statistics for Scientists and Engineers* (McGraw-Hill Series in Probability and Statistics)
- [30] Press W H, Flannery B P, Teukolsky S A and Vetterling W T 1992 *Numerical Recipes in C (The Art of Scientific Computing) (Second Edition)* Cambridge University Press
- [31] VTI SCA620-CHCV1A Datasheet (Revision 2/2). Checked on 22.12.2009
- [32] Analog Devices ADXRS300ABG Datasheet (Revision B). Checked on 22.12.2009

## Appendix A. Error analysis of the measured mean angular velocity

Before going on, observe that the rotation angle  $\theta$  is known to be exactly  $2\pi k$ , where  $k \in \mathbb{N}$  is the number of revolutions. This follows from the type of the measurement explained in section three, and it plays a central role in the error analysis.

The measured average angular rate  $\hat{\omega}_{\text{avg}}$  and the true average angular rate  $\omega_{\text{avg}}$  satisfy

$$\delta\omega_{\text{avg}} = \hat{\omega}_{\text{avg}} - \omega_{\text{avg}}, \quad (\text{A.1})$$

where  $\delta\omega_{\text{avg}}$  is the error in the measured mean angular velocity. Similarly for the rotation time  $T$ , it holds that

$$\delta T = \hat{T} - T. \quad (\text{A.2})$$

Now, since the mean angular velocity over a certain time period is defined as

$$\omega_{\text{avg}} = \frac{\theta}{T}, \quad (\text{A.3})$$

$\delta\omega_{\text{avg}}$  can be written as

$$\delta\omega_{\text{avg}} = \frac{\theta}{T + \delta T} - \frac{\theta}{T} = -\frac{\theta\delta T}{T(T + \delta T)}. \quad (\text{A.4})$$

From (A.3) we know that

$$T = \frac{\theta}{\omega_{\text{avg}}} = \frac{2\pi k}{\omega_{\text{avg}}} \quad (\text{A.5})$$

holds.

In order to quantify  $\delta\omega_{\text{avg}}$ , we need to quantify  $\delta T$ . For this, we need to assume that

- internal delay of the optical fork sensor is a constant and
- clock drift of the AD-converter is negligible.

Provided that these assumptions are correct and that the sampling frequency of the AD converter is  $f$ , it holds that

$$\delta T = \frac{t_\epsilon}{f}, \quad -1 < t_\epsilon < 1. \quad (\text{A.6})$$

That is, the error in the rotation time is at most the time between two adjacent samples given by the AD converter.

Putting these together and taking absolute values, we get

$$|\delta\omega_{\text{avg}}| = \frac{|\theta| |\delta T|}{|T| |T + \delta T|} < \frac{|\omega_{\text{avg}}|}{f \left| \frac{2\pi k}{\omega_{\text{avg}}} + \frac{t_\epsilon}{f} \right|}. \quad (\text{A.7})$$

When it holds that  $2\pi k f > |\omega_{\text{avg}}|$  (which will be the case for any reasonable choice of  $f$  and  $\omega_{\text{avg}}$ ), (A.7) can be further reduced to

$$|\delta\omega_{\text{avg}}| < \frac{\omega_{\text{avg}}^2}{2\pi k f - |\omega_{\text{avg}}|}. \quad (\text{A.8})$$

## Appendix B. Error analysis of the measured acceleration

Let us use similar notation as in Appendix A, now treated as vectors. That is, the computed reference acceleration  $\hat{\mathbf{a}}$  and the true reference acceleration  $\mathbf{a}$  satisfy

$$\delta\mathbf{a} = \hat{\mathbf{a}} - \mathbf{a}, \quad (\text{B.1})$$

where  $\delta\mathbf{a}$  is the error in the measured centripetal acceleration. In the following, zero angular acceleration is assumed,  $\boldsymbol{\alpha} \equiv 0$ . Hence, the acceleration of an arbitrary point  $\mathbf{r}$  fixed to the rate table is

$$\mathbf{a} = \ddot{\mathbf{r}} + \boldsymbol{\omega} \times (\boldsymbol{\omega} \times \mathbf{r}). \quad (\text{B.2})$$

Notice that  $\mathbf{r}$  describes the position of the origin of the IMU and the position of a certain sensor with respect to the origin of the IMU is denoted by  $\delta\mathbf{r}$ . These vectors rotate with the rate table.

Putting these together,  $\delta\mathbf{a}$  can be written as

$$\begin{aligned} \delta\mathbf{a} &= \hat{\mathbf{a}} - \mathbf{a} \\ &= \ddot{\mathbf{r}} + \delta\ddot{\mathbf{r}} + (\boldsymbol{\omega} + \delta\boldsymbol{\omega}) \times [(\boldsymbol{\omega} + \delta\boldsymbol{\omega}) \times (\mathbf{r} + \delta\mathbf{r})] \\ &\quad - \ddot{\mathbf{r}} - \boldsymbol{\omega} \times (\boldsymbol{\omega} \times \mathbf{r}), \end{aligned} \quad (\text{B.3})$$

where  $\delta\ddot{\mathbf{r}} \equiv 0$  holds. Exploiting the properties of the cross product, it is possible to derive the following upper limit for  $\|\delta\mathbf{a}\|$ :

$$\begin{aligned} \|\delta\mathbf{a}\| &\leq \|\boldsymbol{\omega}\|^2 \|\delta\mathbf{r}\| + 2 \|\boldsymbol{\omega}\| \|\mathbf{r}\| \|\delta\boldsymbol{\omega}\| \\ &\quad + 2 \|\boldsymbol{\omega}\| \|\delta\mathbf{r}\| \|\delta\boldsymbol{\omega}\| + \|\mathbf{r}\| \|\delta\boldsymbol{\omega}\|^2 + \|\delta\mathbf{r}\| \|\delta\boldsymbol{\omega}\|^2. \end{aligned} \quad (\text{B.4})$$

Assuming that  $\|\delta\mathbf{r}\| / \|\mathbf{r}\|$  and  $\|\delta\boldsymbol{\omega}\| / \|\boldsymbol{\omega}\|$  are small and using the notation from Appendix A, we have

$$\frac{\delta a}{a} = \frac{\delta a}{\omega_{\text{avg}}^2 r} \leq \frac{\delta r}{r} + 2 \frac{\delta\omega_{\text{avg}}}{\omega_{\text{avg}}} + \mathcal{O}\left(\frac{\delta r}{r} \frac{\delta\omega_{\text{avg}}}{\omega_{\text{avg}}}, \frac{\delta\omega_{\text{avg}}^2}{\omega_{\text{avg}}^2}\right)$$

$$+ \mathcal{O}\left(\frac{\delta r}{r} \frac{\delta \omega_{\text{avg}}^2}{\omega_{\text{avg}}^2}\right) \quad (\text{B.5})$$

(B.5) contains terms caused by the physical size of the IMU ( $\delta r$ ) and by the measurement error of the angular velocity ( $\delta \omega_{\text{avg}}$ ). Typically, the first term dominates and thus, as an overall "rule of thumb",

$$\delta a \approx \frac{\delta r}{r} a. \quad (\text{B.6})$$

In practice, this estimate has a tendency to be quite pessimistic. This is because in (B.4), the worst case requires a certain direction for the measurement axis of the respective sensor in addition to orthogonality of  $\delta \mathbf{r}$  and  $\boldsymbol{\omega}$ .